Geosciences and Engineering, Vol. 12, No. 2 (2024), pp. 128–138.
https://doi.org/10.33030/geosciences.2024.02.010

THE INFLUENCE OF GYPSUM QUALITY, AUTOCLAVING TIME AND GRINDING ON THE SETTING TIME OF α--HEMIHYDRATE

ÁRON FÖLDESI[1]*, JÓZSEF FAITLI[2]
[1]**Faculty of Earth and Environmental Sciences and Engineering, University of Miskolc*
aron.foldesi@baumit.hu
[2]*Faculty of Earth and Environmental Sciences and Engineering, University of Miskolc*
jozsef.faitli@uni-miskolc.hu

Abstract: The aim of this work is to model the influence of grinding and gypsum quality on the setting time of α-hemihydrate using the design of experiments (DoE) method. The setting time of the gypsum binder is an important property determined by the particle size distribution of hemihydrate crystals. In this study, the change in particle size and setting time of hemihydrate was observed by varying the particle size and crystal water content of raw flue gas desulfurization (FGD) gypsum, duration of autoclaving and grinding intensity as model parameters.

Keywords: *gypsum, setting time, hemihydrate, particle size, design of experiments*

1. INTRODUCTION

Gypsum is a type of mineral that belongs to the group of hydrous sulfate minerals, the dihydrate of calcium sulfate (DH, $CaSO_4 \cdot 2H_2O$). Calcium and sulfate ions are bound together in ring-shaped units whose three-dimensional arrangement results in tubular structures. The water molecules of the crystal water are incorporated into these tubes. This water is only loosely bound by adsorption, dehydration is possible in all stoichiometric ratios (Feldmann and Demopoulos, 2012).

When gypsum is heat-treated at a temperature of over 90 °C a calcium sulfate-hemihydrate is formed, with the following reaction (Van Diessche et al. 2016):

$$CaSO_4 + 2H_2O + dQ = CaSO_4 + \frac{1}{2}H_2O + \frac{3}{2}H_2O \quad (1)$$

According to the above equation, calcium sulfate hemihydrate is formed in crystalline form by removing three-quarters of the gypsum crystal water.

β-hemihydrate, which is produced by a dry process (e.g. calcination), is a fine crystalline form resulting from the rapid transformation of the dihydrate. The α-hemihydrate (α-HH), the fully formed hexagonal crystal form, is produced by wet heat treatment (e.g. autoclaving) with steam (Yin and Yang, 2020; Guan et al., 2021). The dehydration process can be divided into two phases: the first is the induction period

of α-hemihydrate, in which the crystal water content of the sample changes only slightly, and the second is the crystal growth of α-HH, in which the crystal water content decreases significantly (Fu et al., 2018; Singh et al., 2007). Upon solidification, the α-hemihydrate can form a stronger crystal structure than the β-form, which is why it is mainly used as a raw material for gypsum binders and floor leveling compounds (Levry and Williamson, 1994).

Due to the hydraulic properties of the hemihydrate, rehydration occurs when it is mixed with water, which is the opposite of the previous equation:

$$CaSO_4\frac{1}{2}H_2O + \frac{3}{2}H_2O = CaSO_4 + 2H_2O + dQ \quad (2)$$

The hydration of hemihydrate is a three step process of solving of hemihydrate, dihydrate seed crystal formation and growing of dihydrate beside inner hydration. The hemihydrate dissolves moderately in water (0.65 g/100 ml) and quickly reaches saturation. The solubility of the dihydrate (0.24 g/100 ml) is only a fraction of the solubility of the hemihydrate, but they form crystallization nuclei during the binding reaction, then precipitate and grow rapidly into an interlocking crystalline mass, significantly accelerating the setting time (Levry and Williamson, 1994).

The influence of the particle size of the α-hemihydrate is also important for the setting time. According to the literature, most authors agree that fine gypsum binders with a higher specific surface area set faster (Baohong et al., 2010; Pan et al. 2007).

2. MATERIAL AND METHODS

2.1. Preparation of hemihydrate

During the model experiments, the gypsum binder samples were prepared in a pilot laboratory equipped for the production and testing of α-hemihydrate. The equipment of the experimental laboratory is identical to the production technology for industrial α-hemihydrate, the steps of the process are presented in *Figure 1*.

During test preparation, the gypsum is treated with water, press adhesive (ground α-hemihydrate) and crystal-forming additives in such a way that molded bodies with a defined density for the autoclaving process are produced by pressing, which survive the autoclaving process undamaged. During production, two additives are added to the mixture to promote the formation of α-hemihydrate crystals under hydrothermal conditions.

The technological advantage of the α-gypsum production process lies in the production of raw gypsum blocks with a certain press density. During pressing, test blocks with a weight of ~6.5 kg are produced.

From a crystallographic point of view, the central technological step in the production of hemihydrate from flue gas desulfurization (FGD) gypsum is the pressurized heat treatment in the autoclave, in which the energy required to remove the water of crystallization is provided by the condensation heat of the steam. The α-hemihydrate, which consists of large, dense crystals, can only be produced in the hydrothermal reaction by controlling the temperature and pressure correctly. The

conversion must be carried out in such a way that complete recrystallization takes place in the solution phase. During the experiments, the recrystallization of the hemihydrate was carried out in a Systec D90 autoclave modified for this purpose.

The process objective of drying α-hemihydrate gypsum is to reduce the water physically present in the molded parts to less than 0.5% by weight at the end of the hydrothermal heat treatment. The air temperature is above 110 °C during the entire drying period; however, the surface temperature of the gypsum blocks remains below 100 °C, even though the air temperature is above 100 °C. During the test, the bricks were dried in a Memmert UF110PLUSZ programmable laboratory dryer.

The aim of grinding is to produce a stable and homogeneous α-hemihydrate with a granulometrically defined particle size distribution (PSD) and specific surface area. Grinding was carried out in a Retsch ZM200 centrifugal mill, in which the grinding intensity can be adjusted by setting the rotor speed between 8000 and 18000 rpm.

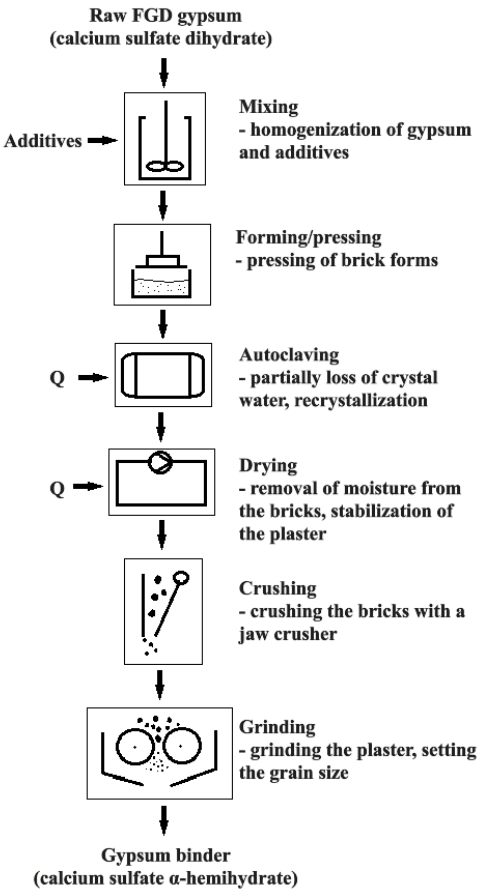

Figure 1
Experimental technology of α-hemihydrate production

2.2. Design of Experiments

The starting material for the model tests was FGD gypsum from the Mátra power plant. The data of the samples used are shown in *Table 1*.

Table 1

Characteristics of the selected gypsum samples

Quality Class	Test No.	Gypsum crystal water [%]	PSD d10 [µm]	PSD d50 [µm]	PSD d90 [µm]	Spec. surface area [cm^2/g]
Poor Crystal Water content between 19.5–19.8%	1	19.58	18.26	47.08	77.94	1205
	2	19.64	18.45	47.21	77.97	1185
	3	19.69	18.24	47.11	77.94	1219
	4	19.54	17.86	46.59	77.33	1233
	5	19.59	18.08	46.35	77.71	1218
	6	19.45	18.29	46.47	77.25	1214
	7	19.59	18.24	47.11	77.94	1219
Medium Crystal Water content between 19.9–20.2%	8	20.14	22.65	48.04	77.54	1178
	9	20.12	22.22	47.88	77.07	1324
	10	19.99	22.53	47.97	77.96	1152
	11	20.08	22.52	48.31	77.92	1199
	12	20.10	22.64	48.29	77.89	1230
	13	20.04	22.69	47.81	77.46	1169
	14	20.05	23.15	48.92	78.55	1283
	15	20.12	22.69	47.81	77.46	1169
High Crystal Water content between 20.3–20.6%	16	20.40	21.42	47.12	75.09	1362
	17	20.36	21.65	47.67	75.69	1356
	18	20.31	21.14	46.7	74.75	1253
	19	20.35	21.17	47.62	75.68	1362
	20	20.42	21.87	47.56	75.39	1355
	21	20.35	21.29	47.57	75.67	1330
	22	20.47	21.17	47.62	75.68	1362

As it can be seen from the table, low-grade gypsum is characterized by a low crystal water content, which is due to the high proportion of inert constituents and the low dihydrate content. These samples also typically exhibited a heterogeneous, broad particle size distribution, with more fine and larger particles. High-quality gypsum, on the other hand, is characterized by high crystal water content and a more homogeneous particle size distribution.

In the DoE study, the particle size distribution (PSD) and the setting time of the α-hemihydrate binder were observed by varying three model parameters in three

stages. The selected parameters were the crystal water content of the raw gypsum, the autoclaving time as independent variables and the grinding intensity (mill speed) as a dependent variable.

The first important step in the design phase was to determine the three levels, as these determine whether the variables have a significant influence on the target values. If the repeatability of these measurements is poor, the error within one experimental set-up will be greater than between two experimental set-ups. If there is no significant difference between the experimental setups compared to the target values, then we cannot say anything about the effect of these input variables. To create the model, a total of 9 experimental setups were defined, with each run repeated once and 4 runs repeated three times to create accurate model equations.

After all the experiments have been carried out, a linear mathematical model is fitted to the target values as a function of the three parameters. The model equation was as follows:

$$y = a_0 + a_1 * x_1 + a_2 * x_2 + a_3 * x_3 \tag{3}$$

The evaluation started by checking the significance of the changes in the model to determine whether they are meaningful changes or just the noise of our measurements. The average variance of the two sets of replicates was taken and used in two-sample t-tests to verify if there was a significant difference between the results. The aim was to perform the regression calculations and determine the best fit using the analytical solution. It had an analytical solution given by the equation below:

$$a_i = (X^T * X)^{-1} * X^T * y \tag{4}$$

X was the matrix of input parameters and y the target values. The calculations provide the values b and a_i of the model equation for the respective target variable. These steps were then repeated with the next target variable. After calculating the values b and a_i, a prediction could be made for each run. Based on the predicted values and the measured values, the performance of the model could be determined. By calculating the values for the total, external and internal variance (residual error), the coefficient of determination (CoD.) and coefficient of correlation (CoC.) of the model could also be determined. The proportion of the total variance that could be explained by the regression was calculated using the explained variance (external variance/total variance).

2.3. Measurement Methods

During the measurements, the crystal morphology of the recrystallized bricks examined with SEM images so that the relationships obtained from the model equations could be better interpreted. A Phenom ProX scanning electron microscope was used to make the images. Since both the raw gypsum and the α-hemihydrate binders were fine powders, the particle size distribution (PSD) and specific surface area were determined using laser diffraction. The setting times were determined using the

standard Vicat method. The Vicat needle is cylindrical and moves in a vertical, scaled guide, penetrating a plaster mass located in a mold. The start of setting time is defined as the time at which the needle penetrates no further than a certain distance (20 mm) from the top of the sample. The end of setting time is defined as the time at which the needle no longer penetrates at all (EN 13279-2:2014; Sleiman et al., 2010).

3. RESULTS

The parameters used in the model and the measured results of the settings are summarized in *Table 2*.

Table 2

Parameters (settings) and measured PSD and setting time values of the model

	Model parameters (Settings)			**Target values (Measured values)**				
Exp. No.	**Gypsum crystal water [%]**	**Auto-claving time [hours]**	**Grinding intensity [10^3rpm]**	**PSD d10 [µm]**	**PSD d50 [µm]**	**PSD d90 [µm]**	**Set. Start [min]**	**Set. End [min]**
1	19.58	6.5	16	2.62	13.60	37.06	4.6	6.6
2	19.64	6.5	16	2.51	13.40	35.21	3.9	5.8
3	19.69	6.5	16	2.37	11.88	31.93	3.9	6.1
4	19.54	7.5	12	2.97	17.00	47.98	6.2	8.4
5	19.59	7.5	12	3.30	17.53	49.15	7.1	8.5
6	19.45	8.5	8	3.70	23.36	59.03	7.08	9.82
7	19.59	8.5	8	3.54	21.55	55.87	6.7	9.5
8	20.14	6.5	12	3.01	16.18	40.48	4.7	6.5
9	20.12	6.5	12	2.95	15.09	39.55	5.0	6.9
10	19.99	6.5	12	2.94	15.62	43.50	4.8	7
11	20.08	7.5	12	2.99	15.47	41.76	5.2	7.4
12	20.10	7.5	12	3.02	14.38	37.32	4.8	6.9
13	20.04	8.5	12	3.09	15.77	41.76	4.8	7.6
14	20.05	8.5	12	3.03	16.53	42.28	4.6	7.5
15	20.12	8.5	12	2.97	17.30	40.25	4.8	6.9
16	20.40	6.5	8	3.51	21.63	49.69	5.3	8.1
17	20.36	6.5	8	3.44	21.33	50.64	5.0	7.9
18	20.31	7.5	12	3.01	16.13	42.76	5.1	7.5
19	20.35	7.5	12	3.00	16.49	42.87	5.1	7.1
20	20.42	8.5	16	2.64	13.09	33.06	3.8	5.6
21	20.35	8.5	16	2.39	12.33	30.31	3.5	4.8
22	20.47	8.5	16	2.41	12.24	30.50	3.3	4.7

The model equations of PSD values and setting time were determined using the measurement results (target values) and model parameters (settings), and then the predicted values were calculated using these equations. The measured and predicted values are summarized in *Table 3*.

Table 3

Measurement and predicted PSD and setting time values

	Measured values					Predicted values				
Exp. No.	**PSD d10 [µm]**	**PSD d50 [µm]**	**PSD d90 [µm]**	**Set. Start [min]**	**Set. End [min]**	**PSD d10 [µm]**	**PSD d50 [µm]**	**PSD d90 [µm]**	**Set. Start [min]**	**Set. End [min]**
1	2.62	13.60	37.06	4.6	6.6	2.52	12.55	35.59	4.6	6.3
2	2.51	13.40	35.21	3.9	5.8	2.51	12.47	35.13	4.5	6.2
3	2.37	11.88	31.93	3.9	6.1	2.51	12.41	34.74	4.4	6.1
4	2.97	17.00	47.98	6.2	8.4	3.08	17.29	46.53	5.9	8.1
5	3.30	17.53	49.15	7.1	8.5	3.08	17.23	46.15	5.8	8.0
6	3.70	23.36	59.03	7.08	9.82	3.65	22.10	57.85	7.2	10.0
7	3.54	21.55	55.87	6.7	9.5	3.63	21.91	56.78	7.0	9.8
8	3.01	16.18	40.48	4.7	6.5	2.97	16.25	41.34	4.7	6.9
9	2.95	15.09	39.55	5.0	6.9	2.98	16.28	41.49	4.8	6,9
10	2.94	15.62	43.50	4.8	7	2.99	16.44	42.49	5.0	7.2
11	2.99	15.47	41.76	5.2	7.4	3.01	16.59	42.38	5.0	7.2
12	3.02	14.38	37.32	4.8	6.9	3.01	16.56	42.23	5.0	7.1
13	3.09	15.77	41.76	4.8	7.6	3.05	16.90	43.28	5.2	7.4
14	3.03	16.53	42.28	4.6	7.5	3.05	16.89	43.20	5.2	7.4
15	2.97	17.30	40.25	4.8	6.9	3.04	16.80	42.66	5.1	7.3
16	3.51	21.63	49.69	5.3	8.1	3.47	20.34	49.39	5.4	8.0
17	3.44	21.33	50.64	5.0	7.9	3.47	20.39	49.70	5.5	8.1
18	3.01	16.13	42.76	5.1	7.5	2.98	16.29	40.62	4.6	6.8
19	3.00	16.49	42.87	5.1	7.1	2.98	16.24	40.31	4.5	6.7
20	2.64	13.09	33.06	3.8	5.6	2.47	11.98	30.31	3.5	5.1
21	2.39	12.33	30.31	3.5	4.8	2.48	12.07	30.85	3.6	5.3
22	2.41	12.24	30.50	3.3	4.7	2.47	11.92	29.93	3.4	5.1

After grinding the experimental hemihydrate bricks, the particle size distribution of the hemihydrate correlates well (coefficient of correlation (CoC.) between 91.8% and 96.7%) with the grinding intensity, and the influence of raw material gypsum quality was also significant. In the experiments, the autoclaving time had no significant influence on the particle distribution values. The model equations defined for the PSD values were as follows:

$$y_{d10} = 6.96 - 0.13 * x_{\text{cw gypsum}} - 0.13 * x_{\text{grinding intensity}} \quad (5)$$

$$y_{d50} = 54.02 - 1.30 * x_{\text{cw gypsum}} - 1.11 * x_{\text{grinding intensity}} \quad (6)$$

$$y_{d90} = 222.24 - 7.67 * x_{\text{cw gypsum}} - 2.52 * x_{\text{grinding intensity}} \quad (7)$$

The equation states that the higher the crystal water content of the gypsum and the higher the grinding intensity, the more widely dispersed the values obtained, i.e. the finer the material. In the equation, the d10 and d90 particle size values of the hemihydrate samples, where the raw material gypsum was of a higher quality class, decreased compared to the results of the lower quality with low crystal water content. Since the specific surface area of the three selected raw gypsums increased with quality, this observation supports the results of Fu et al. (2018). According to their study, the gypsum samples with smaller particle sizes generally had a higher proportion of smaller hemihydrate crystals. The induction time of recrystallization was significantly reduced as the smaller gypsum crystals offer a larger relative specific surface area and more nucleation sites.

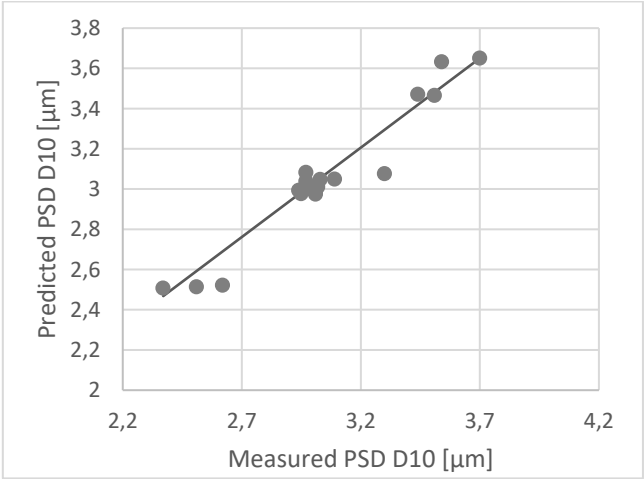

Figure 2
Performance of the d10 model (CoD. = 94.7%, CoC. = 97.3%)

The equation of the d50 model showed an interesting picture, as the median of PSD (d50) increased with increasing crystal water and gypsum quality. The probable reason for this was that the size distribution of the low-quality gypsum had the smallest d10 values and the largest d90 values, so this feature could also influence the particle size of the resulting hemihydrate due to the wide distribution. This was also confirmed by the SEM images of the crystal morphology of the hemihydrate. As can be seen in the images, the hemihydrate produced from low-quality FGD gypsum was a heterogeneous system consisting of needle-like and larger crystals, while the α-

hemihydrate produced from gypsum with a high crystal water content formed a more homogeneous system consisting mainly of developed crystals. Therefore, the particle size of the hemihydrate was more uniform and the size consistency better when it was produced from high-quality gypsum with a higher amount of crystal water.

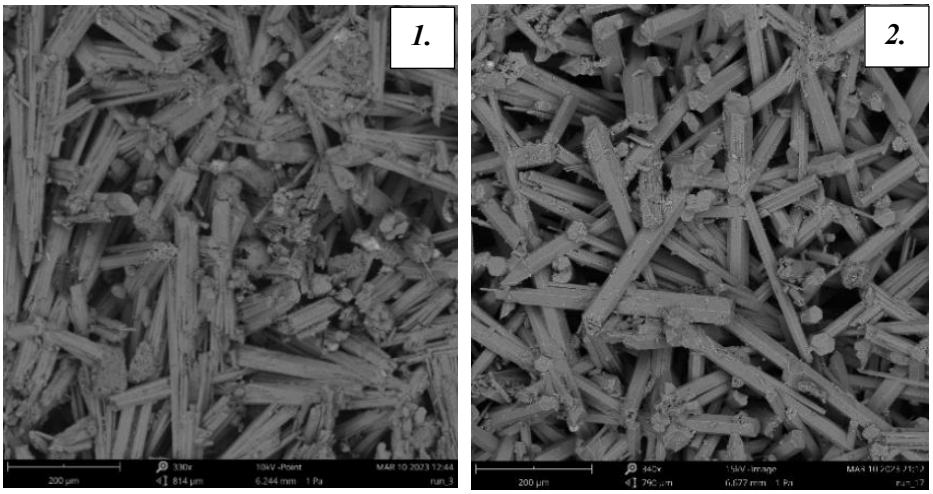

Figure 3
SEM Pictures of HH, 1. from low-quality; 2. from high-quality gypsum

The results of the setting time model show that the setting times are accelerated if we increase the mill speed (rpm) and thereby increase the specific surface area of the α-hemihydrate. The crystal water content of the FGD gypsum was also significant; the effect was negative according to the model, i.e. increasing it accelerated the setting time. The equation for the start and end of the setting time was as follows:

$$y_{set.\ time\ start} = 39.66 - 1.62 * x_{\text{cw gypsum}} - 0.27 * x_{\text{grinding intesity}} \quad (8)$$

$$y_{set.\ time\ end} = 45.83 - 1.74 * x_{\text{cw gypsum}} - 0.40 * x_{\text{grinding intesity}} \quad (9)$$

For this reason, according to the model, hemihydrate from a higher quality class leads to faster setting. In addition, the model showed that an inferior α-hemihydrate with low crystal water content and a larger particle size range generally sets more slowly.

4. DISCUSSION AND CONCLUSIONS

As part of the DoE, a total of 9 settings were defined to create the model and a total of 22 repeat tests were carried out. The equations were set up reliably and with good performance.

According to the equations, the quality of the raw material and the grinding intensity (grinding speed) significantly influence the particle size distribution (PSD). Hemihydrate made from high-quality gypsum had a finer and more uniform particle

size consistency (steeper PSD). The autoclaving time had no significant influence on the particle size values at these setting levels.

In the second part of the study, we were able to model the setting time in good correlation (CoC. between 90.5% and 96.0%) with the crystal water content of the raw gypsum and grinding intensity. The model equation for the setting time showed that the crystal water content of the α-hemihydrate has the greatest influence, but the grinding intensity also plays an important role. Hemihydrate binders with higher water content, which are produced at a higher mill speed, generally have faster setting times.

Due to the closure of power plants in the course of decarbonization, the availability and affordability of FGD gypsum are continuously decreasing. As FGD gypsum is one of the main raw materials for gypsum binders, the industry might be forced to use lower-quality gypsum. The α-hemihydrate is one of the materials most affected by this problem in the gypsum industry, as one of the basic requirements for sufficient and controllable recrystallization in autoclaves is high gypsum quality and thus the lowest possible inert content. The aim of this study is to investigate that this limitation can unfortunately affect important gypsum binder properties such as setting time and particle size. Eliminating such effects and maintaining a stable binder quality could therefore be one of the most important technical challenges for the gypsum industry in the future.

REFERENCES

Van Driessche, A , Stawski, M. , Benning, L. and Kellermeier M. (2016). Calcium Sulfate Precipitation Throughout Its Phase Diagram. *New Perspectives on Mineral Nucleation and Growth, Springer*, pp. 227–231. https://doi.org/10.1007/978-3-319-45669-0_12

Lewry, A. J. and Williamson, J. (1994). The setting of gypsum plaster Part I The hydration of calcium sulphate hemihydrate. The setting of gypsum plaster Part III. The effect of additives and impurities. *Journal of Materials Science*, 29, pp. 5279–5284, 6085–6090. https://doi.org610.1007/BF01171536

Yin, S. and Yang, L. (2020). α or β?-hemihydrates transformed from dihydrate calcium sulfate in a saltmediated glycerol–water solution. *Journal of Crystal Growth*, 5050, 125885. https://doi.org/10.1016/j.jcrysgro.2020.1258855050

Baohong, G., Qingqing, Y., Zhongbiao, B., Wenbin, L. and Liuchun, Y. (2010). Analysis of the relationship between particle size distribution of α-calcium sulfate hemihydrate and compressive strength of set plaster- Using grey model. *Powder Technology*, 200, pp. 136–143. https://doi.org/10.1016/j.powtec.2010.02.015

Pan, H., Deng-xing, L., Peng-sheng, W. and Zhi-ming, T (2019). Effect of Particle Size Ratios on the Physical and Chemical Properties of Surgical-Grade Calcium Sulfate Hemihydrate. *Orthopaedic Surgery Volume*, 12, pp. 1–7. https://doi.org/10.1111/os.12569

Singh, N. B and Middendorf, B. (2007). Calcium sulphate hemihydrate hydration leading to gypsum crystallization. *Progress in Crystal Growth and Characterization of Materials*, 53, pp. 57–77. https://doi.org/10.1016/j.pcrysgrow.2007.01.002

Sleiman, H., Perrot, A., and Amziane, S. (2010). A new look at the measurement of cementitious paste setting by Vicat test. *Cement and Concrete Research*, 40, pp. 681–686. https://doi.org/10.1016/j.cemconres.2009.12.001

Guan, Q., Sui, Y., Zhang, F., Yu, W., Bo, Y., Wang, P., Peng, W., and Jin, J. (2021). Preparation of α-calcium sulfate hemihydrate from industrial byproduct gypsum: a review. *Physicochemical Problems of Mineral Processing*, 57, pp. 168–181. https://doi.org/10.37190/ppmp/130795

Feldmann, T. and Demopoulos, G.P. (2012). Phase transformation kinetics of calcium sulfate phases in strong CaCl2-HCl solutions, Hydrometallurgy, 129, pp. 126–134. https://doi.org/10.1016/j.hydromet.2012.08.015

Fu, H., Jia, C., Chenb, Q., Caoa, X. and Zhang X. (2018) Effect of particle size on the transformation kinetics of flue gas desulfurization gypsum to α-calcium sulfate hemihydrate under hydrothermal conditions. *Particuology*, 1084, pp. 1–7. https://doi.org/10.1016/j.partic.2017.10.004

EN 13279-2:2014. *Gypsum binders and gypsum plasters - Part 2: Test methods.*